Proceedings of the IASS 2024 Symposium
Redefining the Art of Structural Design
August 26-30, 2024, Zurich Switzerland
Philippe Block, Giulia Boller, Catherine DeWolf,
Jacqueline Pauli, Walter Kaufmann (eds.)

Curve-Fit, Free-Form Timber Structures through Curved-Folded Modules

Alan ESKILDSEN*, Pinaki MOHANTY[a], Carolina Leite VIEIRA[b], Simon BECHERT[c], Axel KÖRNER[d], Jan KNIPPERS[e]

*ICD & ITKE, Universität Stuttgart
Keplerstraße 11, 70174 Stuttgart, Germany
contact@alaneskildsen.com

[c, d, e] ITKE, Universität Stuttgart

Abstract

Free-form timber structures are currently a high interest topic that represents a limited niche within the AEC industry and a resource intensive choice for building. This research explores an alternative to current technologies for their production through "Curve-Fit", a building system that uses flat-packed timber modules that can be transformed through curved-folding. Transformed modules are connected along curved creases to form load bearing structures. A set of strategies were developed for the geometric design, structural validation and detailing of the system. These were wrapped in an integrated feedback workflow for the informed coordination of multiple design objectives. The system was tested with a full scale demonstrator, proving that load bearing structures can be produced with the Curve-Fit system. The proposed strategies have the potential to increase production efficiencies and reduce resource consumption in the production of free-form timber structures.

Keywords: curved folding, bending-active, timber, flat-pack, transformative structures, deployable structures, finite element analysis, optimization, free-form, lightweight structures

1. Introduction

Timber has regained popularity as a structural material due partly to its environmental advantages. This in tandem with design trends that favor expressive and performative characteristics has led to timber structures that showcase a range of free-form geometries. (Section 1.2)

However, the production of timber components for free-form structures is still complex and resource intensive. For instance, producing curved Glulam, a system commonly used for structures such as gridshells, "involves techniques such as subtractive milling-to shape or extensive formwork and machines to bend, press, and glue thin timber lamellas to the desired curved shapes." (Grönquist [3]). Additionally, the storage, transportation and handling of curved components leads to lower efficiencies at various stages of production when compared to linear elements.

The use of bent-active and curved-folding components represents a sustainable and economical alternative for these structures, since variable geometric characteristics can be achieved by bending and folding initially flat timber elements. To achieve this, designs must be adapted to the geometrical rules of these surfaces and to the physical constraints of bending an anisotropic and thick material. Foremost, developing connection strategies between plates and other components becomes a crucial consideration for achieving safe and stable structures that can be efficiently produced and swiftly assembled.

1.2. State-of-the-Art Work

Three main variants from related work serve as primary precedents to the Curve-Fit system:

1.2.1 Timber buildings with free-form structures. Of note is the Haesley Nine Bridges Golf Club by Shigeru Ban (2009) and the Cambridge Mosque by Marks Barfield (2019), which feature curved glulam gridshell structures that allow open spatial arrangements as a result of their column supports.

1.2.2 Geometric research on curved-folding structures. "Interactive Design of Curved Crease-Folding" (Bhooshan, S. [2]) presents a process to form-find trivalent curved-folding assemblies and was physically tested with aluminum formworks. "Curved folded cone assemblies" (Maleczek, R. et. al. [8]) presents a system structured through curved-folded modules that are connected along curved-creases, and was tested through a pavilion made from paper.

1.2.3 Research on full-scale structures using curved-creased connections, such as the "Curved Folding Bridge" (Maleczek R. et al. [9]) and "Timbr Foldr" (Başnak, O. et. al. [11]). Both use plywood as a structural material and fabric and belt straps respectively for hinges in curved-folding connections. "Spatial Developable Meshes" (Bhooshan V. et al. [1]) and "Active Timber" (Krieg, [13]) have presented methods for assembling bent plates along curved-crease connections, respectively using fibers and dowels. Most of these systems achieve a limited geometric freedom due to the constraints imposed by the use of thick timber plates.

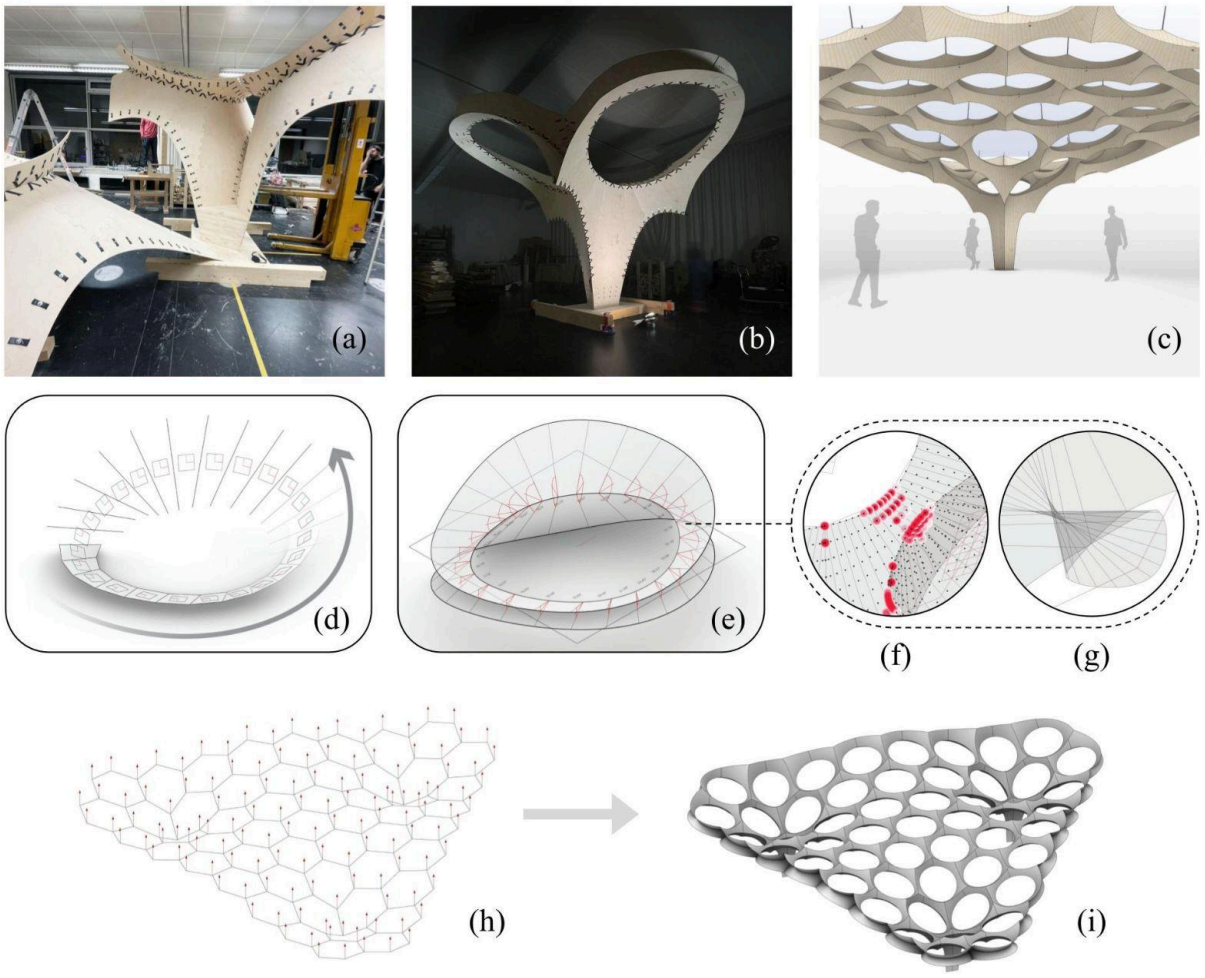

Figure 1.(a) Prototype assembly; (b) Built Prototype; (c) Envisioned application of the system; (d) Tangential Plane Surface Modeling for CFM; (e) Stacked-Curved Folding Constraint; (f) Detection of curvature anomalies; (g) Surface self intersection; (h) Hanging chain model, (i) CFM surface model supported by columns.

1.3. Scope

The primary research objectives with this system included: (1) investigating strategies for planning with a modular building system of transformable timber components; (2) pointing at relevant configurations of the system with free-form geometries and open plans enabled by column supports; and (3) developing structural validation and production methods for load-bearing structures.

The proposed Curve-Fit system (Figure 1a - c) is composed of Conoid Folding Modules (CFMs), which can be produced and transported in a flat state and transformed to a tridimensional configuration before their assembly into a larger structure. Each CFM has two plywood plates connected along a curved hinge. The modules can be quickly transformed to a tridimensional configuration by pulling on their open edges, which results in a curved folding actuation. Free-form load bearing structures composed of hollow polygonal elements can be assembled by connecting transformed CFMs along curved creases, further rigidizing the system. Additionally, such structures can be swiftly disassembled at the end of their lifespan allowing efficient salvaging and re-use of their components.

4. Methodology

4.1. Local Design Framework

To control the variable dimensions of each structural element, tangential surfaces were used for the geometry of each plate in the CFM's. This framework involves the modeling of developable surfaces with curved-folding creases and the detection of unwanted features that affect interrelated constraints.

4.1.1. Tangential Plane Surface Modeling. Developable surfaces intrinsically have zero Gaussian curvature at any point (Lawrence,S. [5]). Following a similar procedure to the one in Bo & Wang [12] , an input surface serves as a design guideline to which a tangential surface is approximated. A set of consecutive normal planes are sampled on the guideline surface at constant intervals, and a set of new tangential ruling lines is found through the sequential intersection of these planes. An approximation surface can be modeled through the resulting intersection curves (Figure 1d).

4.1.2. Curved-folding reflection modeling. At any point on the curved-fold, the resulting angle between rulings from opposite surfaces should be equal across the osculating plane on the curve (Vergauwen A. et. al. [10]). Therefore the stacked curved-folding surfaces of the CFM's are defined through the reflection of developable surfaces across the base plane where the hinge is located (Figure 1e).

4.1.3. Detection of surface anomalies. This process captures instances where geometric and physical limitations have been exceeded. These include: (1) non-zero gaussian curvatures; (2) self-intersecting surfaces determined by intersections between ruling lines within the boundary of the surface; and (3) zones where the curvature of the material is higher than the maximum permissible curvature.The reduction of anomalies can be achieved by increasing the resolution of ruling lines in the case of non-zero gaussian curvatures, or by modifying the module's geometry when self-intersections or maximum curvatures are detected (Figure 1 f - g).

4.2. Global Design Framework

The system's global design involves the modeling of multiple CFMs and their strategic placement. Parameters such as (1) the angles between neighboring module's base planes; (2) the distance between hinge curves; and (3) the angles between the rulings of each plate and the base plane of their parent module contribute to the shaping and dimensions of each structural component and curved-creased connections. As a result, multiple characteristics can be achieved at the global level with the same system, from spatial arrangements supported by columns to a variety of geometric configurations. Two modeling strategies were developed for the generation of global geometries:

4.1.2. Hanging Chain Model. column elements are modeled through the extension of nodes between modules. Linear structural elements are traced in a planar configuration, with polygonal cells serving as a boundary guide for each pair of CFM's surfaces. Anchors placed on the expected support locations allow the coordinated inclination of neighboring modules into concave zones during the

loading of the model, which forces the extension of surfaces that form the column elements. The model is increasingly loaded. converging once the columns reach acceptable sections (Figure 1h - i).

4.1.2. Module Population: here a surface is taken as an environment to place the CFMs through a particle flocking simulation, which distributes the polygonal cells on which CFMs are modeled. The aim with this approach is to reach an even distribution of modules on the structure while avoiding significant variations that could result in unattainable bending radiuses.

4.3. Material feasibility - Timber plywood

Materials used for bending active structures should be able to bend to the desired curvature and resist external loads in the bent state. These generally have a ratio $\sigma_{M,Rk}/E > 2.5$ (where $\sigma_{M,Rk}$ is flexural strength in MPa and E is the elastic modulus in GPa) (Lienhard, J. et. al. [6]). The ratio for birch plywood is around 4, and therefore has been chosen as a material for exploration in this research.

4.3.1. Grain direction: Plywood is an orthotropic material where the modulus of elasticity is higher along the grain direction. Consequently, one can achieve a higher curvature when bending it across the grain direction. This phenomenon is best explained using the well known Euler Bernoulli equation, which relates allowable stress to bending curvature and young's modulus.

4.3.2. Segmentation: In an ideal scenario, the grain direction must exactly coincide with the ruling lines of the surface, which is impossible with plywood where the grain directions follow a parallel direction. However this can be partially overcome by splitting the plate into multiple segments. A higher segmentation reduces the deviation between grain direction and the ruling lines but undesirably increases the number of joints, introducing more discontinuities in the structure (Figure 2b).

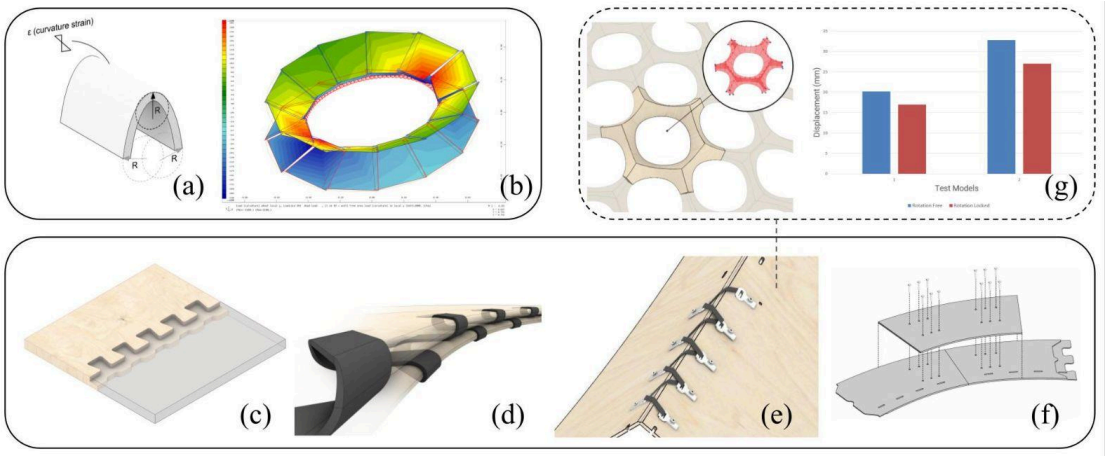

Figure 2: (a) Curvature strain concept; (b) Curvature strains applied to segmented conical module; (c) Plate to plate connection, (d) Hinge connections, (e) Module to Module connection, (f) Module closing connection; (g) Qualitative analysis to study the influence of joint rigidity on the performance of a complete module.

4.4. Connections

Six resilient connection strategies were developed to accommodate bending motions, the reduced section of the plates, varying angles between plates and to achieve a swift assembly and disassembly of the structure. The first two connections were adapted from previous research by Başnak et al, [11].

4.4.1. Plate to Plate (P2P): The P2P is used to accurately align and connect plywood segments into a single plate with varying grain directions. It is a stepped connection, allowing an overlap between segments with interlocking puzzle-joints taking tension forces during bending, and a zig-zag joint in the compression side taking in-plane shear forces (Figure 2c).

4.4.2. Hinge: The hinge is a knitted connection that ties the plates of each CFM with a fabric belt wrapped in an 8 loop pattern. It is anchored to slits on each plate, taking tensile forces and allowing rotation movements during the transformation of the modules (Figure 2d).

4.4.3. Module to Module (M2M): allows the swift connection between multiple CFMs along curved-creases. It is placed by manually weaving a fabric belt through metallic rings anchored to neighboring plates. This connection can only be accessed from one side while allowing minimal adjustments to the position of the modules (Figure 2e).

This connection was developed after conducting a qualitative study to determine the influence of rotational rigidity in the M2M connections. A complete module with adjoining nodes was isolated and tested under an applied load. It was observed that the rotational rigidity of joints had a low impact on the overall performance. This can be attributed to the fact that loads are resisted by in-plane membrane forces due to deformation compatibility (Figure 2g).

4.4.4. Module closing: bolted lap connections enable the locking of the CFMs to a tridimensional state after their transformation. Lap segments are pre-placed on an open end of plates and connected to the opposite one by aligning the pre-milled bolt holes on the plates. This connection is designed to take moment, vertical shear, in-plane shear and the in-plane tensile forces of the plates (Figure 2f).

4.5. Production Framework

A set of minimum infrastructural requirements were devised for an off-site factory environment that produces CFMs in a flat state and ships them to a construction site, where these are subsequently transformed and assembled into a structure.

4.5.1. Off-site Fabrication consisting of the following stations: (1) milling, where a 3-axis CNC machine mills and details the segments from raw plywood panels; (2) glue-application, where glue is applied on the P2P joints, potentially by a machine with a glue end-effector; (3) panel assembly, where segments are assembled for producing individual plates; (4) detailing, where the anchors for the M2M are connected to the plates and pairs of plates are connected with the hinge; and (5) loading, where the assembled CFMs are stacked on a container vehicle for shipping to site.

4.5.1. On-site Assembly consisting of: (1) un-loading, where the CFMs are lifted from the container; (2) optional storage; (3) transformation, where CFMs are individually lifted, transformed to their tridimensional state and locked with the closing connection (Figure 3a); and (4) assembly, where the CFMs are connected with the M2M connection building up the structure (Figure 3b).

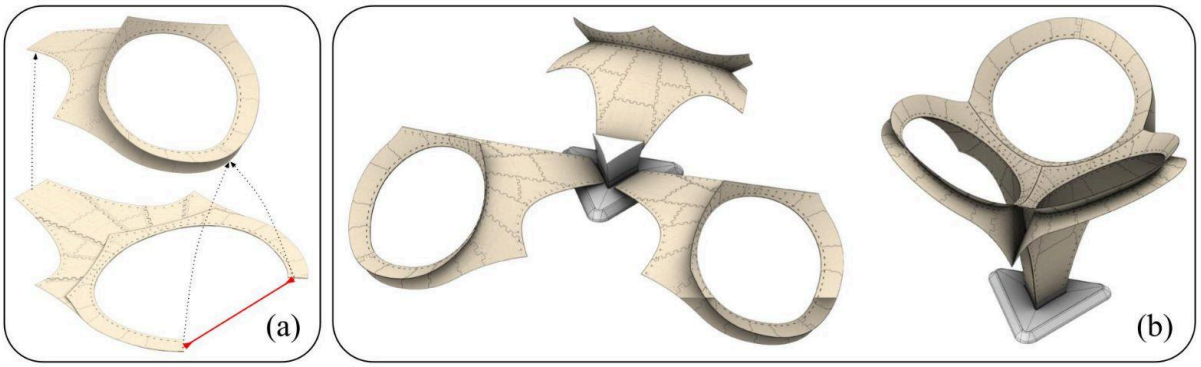

Figure 3: (a) CFM transformation from Flat-Pack to Tridimensional State; (b) Demonstrator Assembly

5. Results

5.1. Full Scale Demonstration Study

A full-scale prototype was built to test the developed methodologies. It consists of 3 radially symmetrical CFMs, and is conceptualized as the transition between the column and canopy portion of a gridshell structure, showcasing its potential for building free-form timber structures (Figure 3).

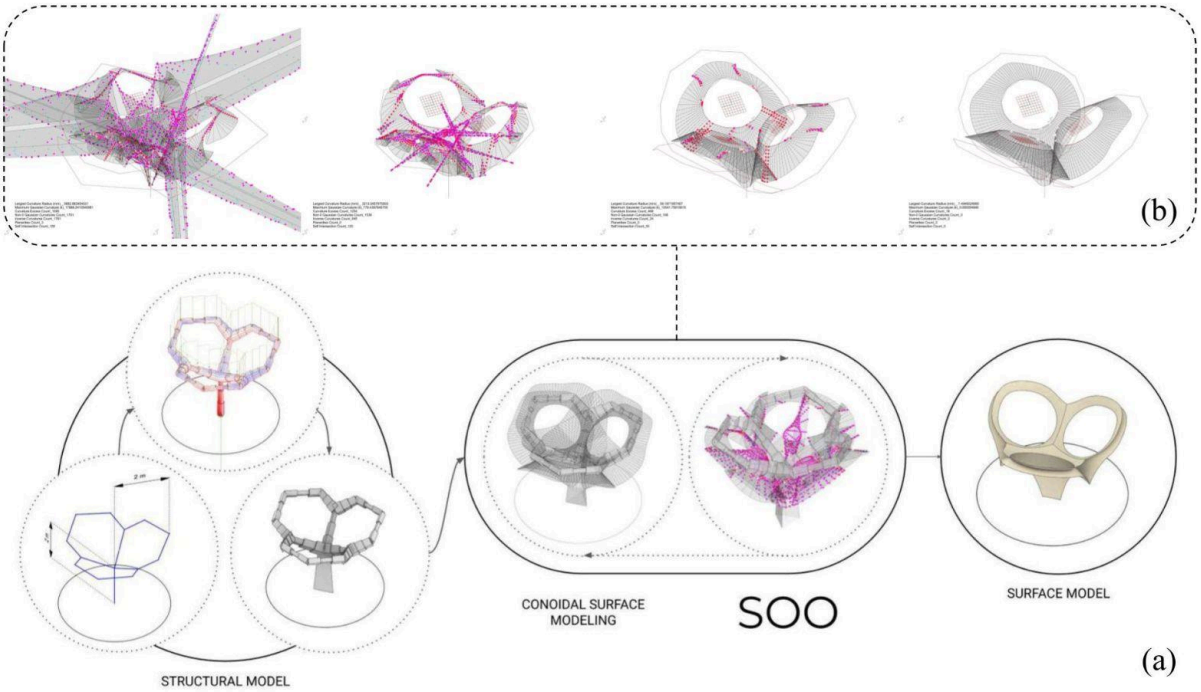

Figure 4: Top: (a) Design workflow for the final demonstrator. Bottom: (b) SOO for surface modeling

5.2. Integrated Workflow

An integrated feed-back workflow was established to coordinate the prototype's concept with the local design framework (section 4.1.) and the physical constraints of the chosen material (Figure 4).

5.2.1. Cross-section optimization: provides a guideline for the elements' dimensions. A simplified Finite Element Model (FEM) with a vertical column element and 3 hexagonal cells representing CFM's are used. The cells are pre-dimensioned to accommodate an approximate bending radius of 175 times the plate's thickness leaving a reserve strength of 30-40% after bending. Beam elements were modeled using hollow circular cross-sections with a thickness of 6.5 mm and were conservatively loaded with 2 kN/m. The beam and columns were assigned different material properties to account for the changing grain directions on the plates in relation to the line model (Table 1), with stresses perpendicular to the grain in horizontal elements and along the grain in vertical elements.

Table 1: Parameters for initial structural analysis.

Parameters	Beams	Columns
Density (kN/m3)	6.8	6.8
Young's modulus (N/mm2)	4763 (Grain perpendicular)	9844 (Grain parallel)
Maximum compressive strength (N/mm2)	29.3	42.2
Maximum Tensile strength (N/mm2)	29.3	29.3

The cross-section optimizer in Karamba 3D was run to arrive at a set of guide cross-sections. The target objectives were a material utilization (von-Mises hypothesis) of 0.75 and a displacement limit of span/150. The circular cross-sections were converted to equivalent diamond sections to more closely fit the section geometries of the system. Figure 4a illustrates the complete workflow.

5.2.2. Single Objective Optimization (SOO): was formulated to find a feasible configuration of the prototype that most closely fits a set of ideal structural sections. An optimization solver was given control over the generation of the CFMs tangential surfaces (section 4.1.1.), constraining their design space to exclusively produce sections larger than the guideline diamond sections (section 5.1.1.).

The following objectives were established with the purpose of achieving a working configuration of the prototype that utilizes the least amount of material: (1) minimizing the total surface area; (2) maximizing the curvature on surfaces; and (3) minimizing planar zones. These were merged into a single objective as all of these values are linearly related.

A set of penalty instances were defined for cases in which the geometry of the surfaces present the anomalies outlined in section 4.1.3. To visually supervise the process, color tags were placed on the probes to indicate the locations where penalties are detected (Figure 4b)

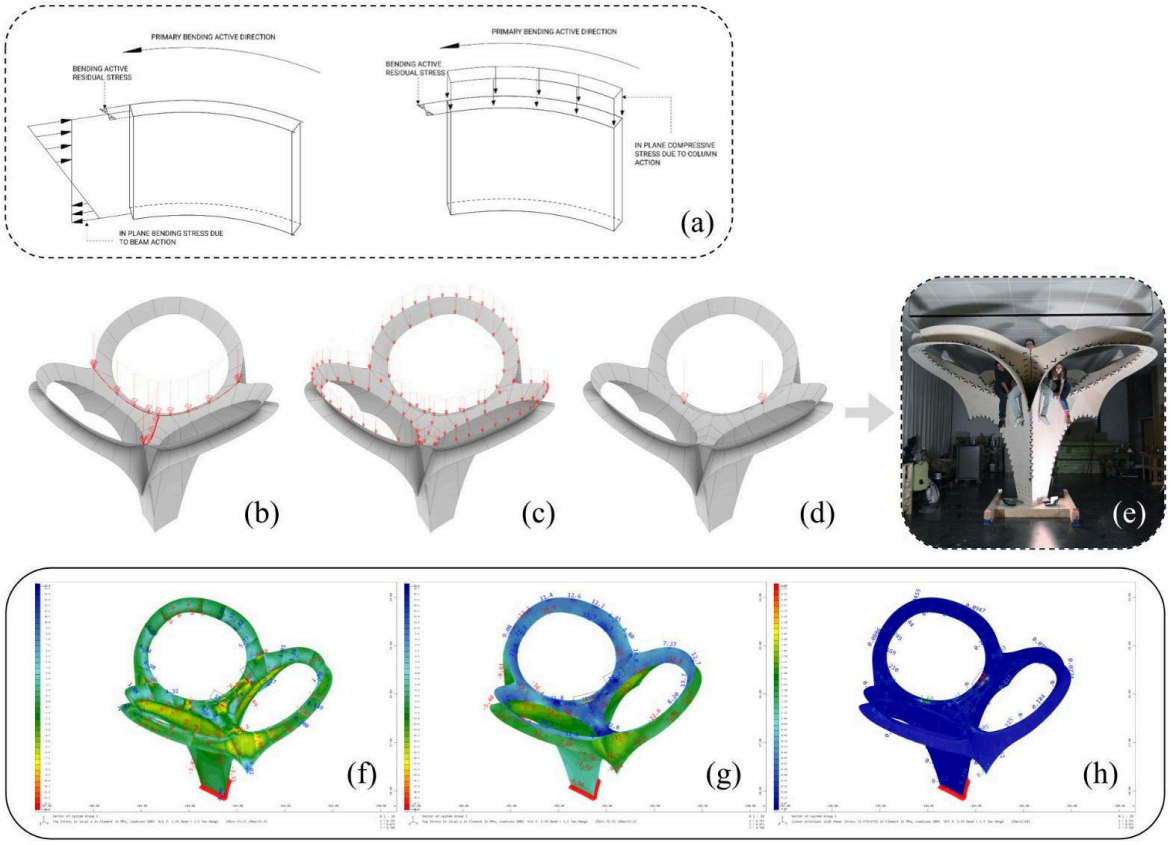

Figure 5: (a) Stress action in a typical element from beam and column regions; (b) Line load of 1kN/m on top crease lines; (c) Area load of 0.2 kN/m² on top; (d) Two 1 kN loads accounting for people hanging from two beams; (e) Human load test on the built demonstrator; (f) σ_x top along the grain; (g) σ_y top (perpendicular to the grain); (h) τ_v

5.3. FEM Modeling

Structural verifications for the prototype model were conducted using a detailed finite element model in Sofistik.

5.3.1. Surface elements: Plywood is modeled as an orthotropic material using quad elements (Figure 2b). Each of the cone strips are divided into 16 segments to achieve a radial grain direction. Material properties as defined in Table 1 were used.

5.3.2. Connections: Hinge and M2M connections are visualized as springs with stiffness k = AE / L; where, A is the cross-sectional area of the strap, E is the modulus of elasticity and L is the inclined length. These inclined springs are mathematically converted into equivalent vertical springs having certain axial and lateral stiffness as required in the FEA model. (Figure 6a)

5.3.3. Load Combinations: Residual stresses due to bending are captured by applying curvature strains Figure 2b illustrates the method for a single module. This method was in contrast to the cable

contraction method developed by La Magna [4] and Lienhard [7] for bending active structures which in addition to evaluating stresses also served as a tool for form finding shapes. Since in the current research the shape is the result of geometry and curved line folding which is known a priori, a more simplified approach was adopted. Additionally, the dead weight of the system and three live load cases are considered as shown in Figure 5 b - d . ULS and SLS Load combinations as per EC0 are evaluated

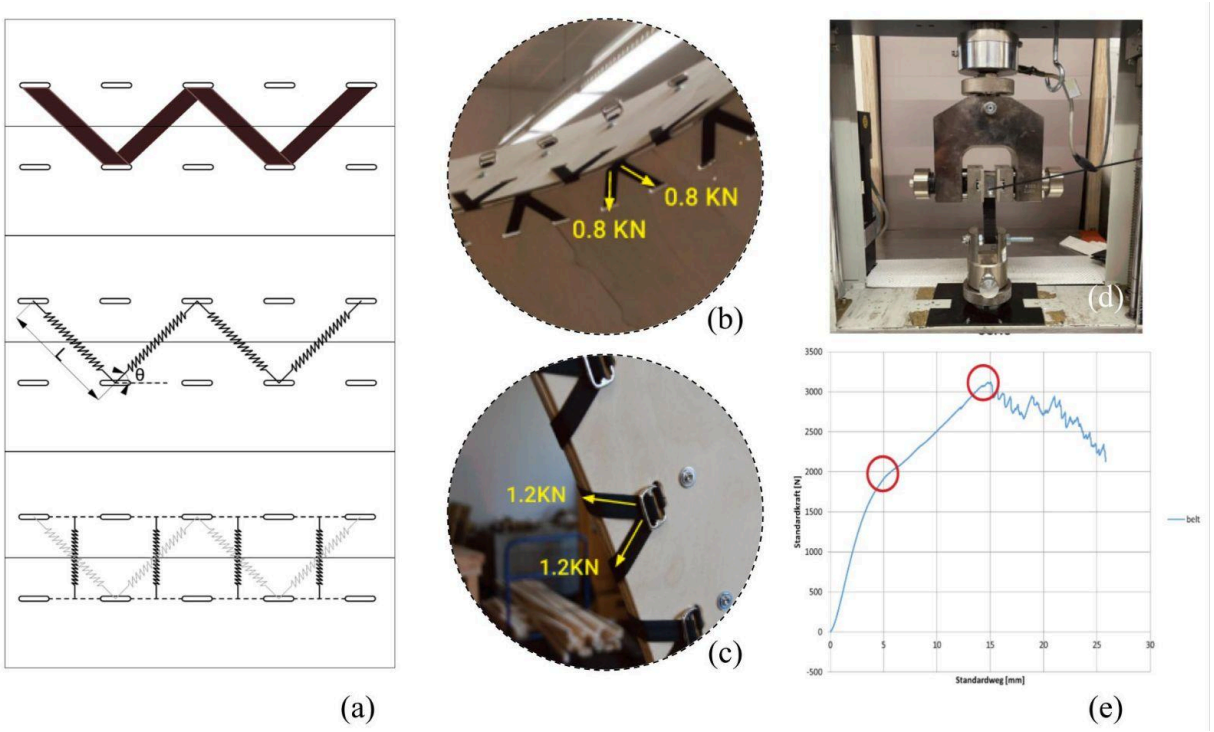

Figure 6: (a) Modeling of connections using springs in the FEA model; (b) Forces in the hinge connection; (c) Forces in the M2M connection; (d) Tension testing of the cured sample specimen; (e) Tension test result.

5.4. Structural verifications for Final Prototype

5.4.1. Stress verifications for plywood: Stresses in plywood are checked for combined axial and bending as per EC5. Since the surfaces are essentially zero gaussian surfaces, bending along the ruling lines will never occur and hence the bending terms in the other direction have been dropped out from the equations. For brevity only the FEA results from top longitudinal stresses and out of plane shear stresses are shown in Figure 5 f - h.

5.4.2. Stability Checks: A buckling eigenvalue analysis was carried out for the final demonstrator to check for global stability. The lowest buckling factor was found to be 1.03 and being greater than 1, no further checks were done.

5.4.3. Webbing and bolt design: The design forces in the webbing and bolts are summarized in Figure 6 for the hinge and M2M connection. In case of M2M connection, the forces from the webbing strap to the bolts are transferred by means of a steel hook attached to a connecting strap. The connecting strap is punched to allow the bolt to pass through which significantly weakens it and might cause the belt to rip apart. In order to strengthen it, the belts were treated with resin and cured in a temperature controlled environment for 5 days. The strengthened connecting strap was tested for its capacity in a tension testing machine (Figure 6d - e). The ultimate capacity ($F_{capacity}$) was found to be as 3 kN. Using a material factor of safety of γ = 1.2, the proof for the connecting strap is as follows.

$$\sqrt{2}.\ F_d\ =\ 1.7\ kN\ <\frac{F_{capacity}}{\gamma}\ =\ 2.5\ kN$$

5.5. Final Prototype Production

The fabrication of the prototype applied the production framework described in section 4.5. with university workshops as fabrication space and construction site (Figure 1a, 3 and 7).

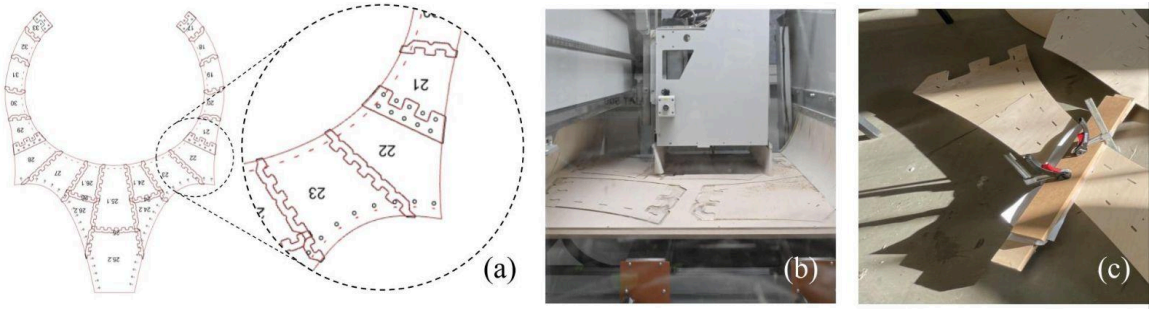

Figure 7: (a) Fabrication milling paths of a single module; (b) 3-axis CNC milling of the segments from plywood; (c) Gluing of individual segments.

5.5.1. Fabrication: Each of the plates was produced from 16 individual segments. This was determined according to structural verifications and the available nesting area in 1.2m X 2.4m plywood panels.

The segment milling was conducted with a 3-axis CNC machine, executing the following paths per plywood plate: (1) vertical drilling for M2M bolt connection openings; (2) linear opening milling for the hinge and M2M belt connections; (3) half thickness milling for the P2P joints; and (4) outline milling for the curved-creases, M2M and hinge creases. The machine counted with automatic drill bit switching, which allowed the swift execution of the fabrication paths one after another (Figure 7a - b).

5.5.2. Plates and Module Assembly. The assembly of the plates was executed manually by: (1) applying standard timber glue on the step portions of the P2P joints; (2) connecting the segments of the plates and pressing the connections on clamp tables for 6 hours until the the glue dried; (3) rounding the edges of the creases and the openings of the M2M and hinge connections (Figure 7c).

5.5.2. Prototype Assembly. The structure was assembled manually by: (1) transforming the CFMs to a tridimensional state; (2) locking the modules with the closing connection; (3) screwing the CFMs to a solid timber base; (4) connecting the CFMs along their open edges with the M2M connection.

6. Discussion

A system is proposed for building free-form timber structures from CFMs. The proposed frameworks can enable the planning and production of these structures by providing a range of geometric design methodologies, structural calculations, construction details and production considerations.

A final demonstrator representing a portion of a larger structure was designed and built to test the developed methods. Each of its three modules could be transformed in seconds, with the closing connection taking about 10 minutes. The final assembly took around 5 hours, a reasonable time considering the process was conducted manually by a group of students, in a limited area and with no lifting equipment. It is expected that in a building site the assembly of structures to be faster when using lifting equipment and a skilled workforce.

Certain limitations were also encountered: (1) It was observed that the belt straps in the M2M connections, although easy to weave, proved difficult and ineffective to tension manually. A new strategy for tensioning could be developed to avoid the need for this manual effort. (2) The flat state of the column module, although compact in terms of thickness, was large in its planar dimensions. These modules could be further subdivided through additional intermediate joints to fit in compact containers. (3) Further scaling the system would also require the use of thicker sections on the plates. Multi-layer plates joined together by railed connections that allow bending could be explored further. (4) The resulting structure would require an additional facade system to provide an enclosed space.

Acknowledgements

This paper is based on the research conducted by the first three authors with the tutoring of the fourth and fifth authors and the academic supervision of the sixth author during the ITECH M.Sc. Thesis Course 2021 - 2022 at the University of Stuttgart. This research was partially supported by Drees & Sommer GmbH and the Institute for Machine Tools (IfW), who respectively provided the funding and infrastructure for the fabrication of the final prototype. The authors would like to acknowledge Prof. Achim Menges for his comments and guidance, Prof. M. Koch, W. Heydlauffrom, M. Schneider, V. Meier and M. Schneider for their invaluable support, and our dear ITECH colleagues A. Simpson, A. Durmaz, C. Kang, C. Blum, G. Muñoz, I. Voineag, K. Amudhan, K. R. Venkatachalam, M. Jafari and P. Castel who wholeheartedly aided in the production of the final prototype.

The authors declare no conflict of interest that could have influenced the work presented in this paper.

References

[1] V. Bhooshan, H. Louth, L. Bieling, and S. Bhooshan, “Spatial Developable Meshes: Mouldless Bent Wood and Seam Winding for Spatial Structures”, in C. Gengnagel et al. (eds) Impact: Design With All Senses. Cham: *Springer International Publishing*, pp. 45–58, 2020.

[2] S. Bhooshan, “Interactive Design of Curved‐Crease‐Folding”, M.Phil. Thesis, Dept. Arch. and Civil Eng., Univ. Bath, Bath, Somerset, 2015.

[3] P. Grönquist,. “Smart manufacturing of curved mass timber components by self-shaping”, Doctoral Thesis., Dept. of Civ. Env. and Geo. Eng., ETH, Zurich, 2020.

[4] R. La Magna, “Bending-active plates : strategies for the induction of curvature through the means of elastic bending of plate-based structures”, Doctoral Thesis, Inst. für Trag. und Konst. Ent., Universität Stuttgart, Stuttgart, 2017.

[5] S. Lawrence, “Developable Surfaces: Their History and Application,” Nexus Network Journal, vol. 13, no. 3, pp. 701–714, Oct. 2011.

[6] J. Lienhard, C. Gengnagel, J. Knippers, H. Alpermann “Active Bending, A Review on Structures where Bending is used as a Self-Formation Process”, *International Journal of Space Structures*, vol 28, pp. 187–196, 2013.

[7] J. Lienhard, “Bending-Active Structures”, Doctoral Thesis. Stuttgart : Inst. für Trag. und Konst. Ent., Universität Stuttgart, 2014.

[8] R. Maleczek, G. Filz, C. Scheiber, M. Heimrath, and C. Preisinger, “Curved Folded Cone Assemblies,” in Conf. IASS 2016: Spatial Structures in the 21st Century, Tokyo, 2016.

[9] R. Maleczek, G. Stern, A. Metzler, and C. Preisinger, “Large Scale Curved Folding Mechanisms,” Springer eBooks, pp. 539–553, Aug. 2019

[10] A. Vergauwen, N. De Temmerman, L. De Laet. “Digital modeling of deployable structures based on curved-line folding,” in Conf. Shells, Membranes and Spatial Structures: Footprints, Brasilia, Brasil, 2014.

[11] G. Rihaczek, M. Klammer, O. Basnak, A. Körner, R. La Magna, and J. Knippers, “Timbr Foldr – A Design Framework and Material System for Closed Cross-section Curved Folded Structures,” Journal of the International Association for Shell and Spatial Structures, vol. 63, no. 4, pp. 272–288, Dec. 2022.

[12] P. Bo and W. Wang, “Geodesic-Controlled Developable Surfaces for Modeling Paper Bending,” Computer Graphics Forum, vol. 26, no. 3, pp. 365–374, Sep. 2007.

[13] O.D. Krieg. *Active Timber* [Online]. Available: https://oliverdavidkrieg.com/?p=627